

REPORT DOCUMENTATION PAGE

1a. REPORT SECURITY CLASSIFICATION Unclassified		1b. RESTRICTIVE MARKINGS	
AD-A219 034		3. DISTRIBUTION/AVAILABILITY OF REPORT Approved for public release; distribution unlimited.	
5. MONITORING ORGANIZATION REPORT NUMBER(S) D 3		ARO 26172.1-MS-A	
6a. NAME OF PERFORMING ORGANIZATION State U of NY at Buffalo	6b. OFFICE SYMBOL (If applicable)	7a. NAME OF MONITORING ORGANIZATION U. S. Army Research Office	
6c. ADDRESS (City, State, and ZIP Code) Buffalo, NY 14260		7b. ADDRESS (City, State, and ZIP Code) P. O. Box 12211 Research Triangle Park, NC 27709-2211	
8a. NAME OF FUNDING/SPONSORING ORGANIZATION U. S. Army Research Office	8b. OFFICE SYMBOL (If applicable)	9. PROCUREMENT INSTRUMENT IDENTIFICATION NUMBER DAAL03-88-K-0202	
8c. ADDRESS (City, State, and ZIP Code) P. O. Box 12211 Research Triangle Park, NC 27709-2211		10. SOURCE OF FUNDING NUMBERS	
		PROGRAM ELEMENT NO.	PROJECT NO.
		TASK NO.	WORK UNIT ACCESSION NO.
11. TITLE (Include Security Classification) Low Coast Processing Routes Leading to High-Performance Ceramic Tiles			
12. PERSONAL AUTHOR(S) Vladimir Hlavacek			
13a. TYPE OF REPORT Final	13b. TIME COVERED FROM 9/15/88 TO 12/14/89	14. DATE OF REPORT (Year, Month, Day) Feb 90	15. PAGE COUNT 26
16. SUPPLEMENTARY NOTATION The view, opinions and/or findings contained in this report are those of the author(s) and should not be construed as an official Department of the Army position, policy, or decision, unless so designated by other documentation.			
17. COSATI CODES		18. SUBJECT TERMS (Continue on reverse if necessary and identify by block number)	
FIELD	GROUP	Ceramic Tiles, Structures, Titanium Diborane, Titanium Boride, Titanium Diboride, Composites	
19. ABSTRACT (Continue on reverse if necessary and identify by block number) Production of cheap high-performance ceramic tiles for structural application is an important problem. The search for superior tile exhibits many different facts ranging from establishing routes for manufacturing cheap precursors, through densification to ballistic testing of the material. (continued on reverse side)			
20. DISTRIBUTION/AVAILABILITY OF ABSTRACT <input type="checkbox"/> UNCLASSIFIED/UNLIMITED <input type="checkbox"/> SAME AS RPT. <input type="checkbox"/> DTIC USERS		21. ABSTRACT SECURITY CLASSIFICATION Unclassified	
22a. NAME OF RESPONSIBLE INDIVIDUAL		22b. TELEPHONE (Include Area Code)	22c. OFFICE SYMBOL

UNCLASSIFIED

SECURITY CLASSIFICATION OF THIS PAGE

The main goals of the research were:

- Synthesis of ultrafine sinterable titanium diboride and titanium boride based composites in a combustion regime.
- purification of titanium diboride synthesized by magnesithermal reduction of boric and titanium oxides.
- densification and fabrication of TiB_2 based composites by pressureless sintering and hot pressing.
- ballistic testing of fabricated tiles.

UNCLASSIFIED

SECURITY CLASSIFICATION OF THIS PAGE

FINAL REPORT

PROJECT TITLE: LOW COST PROCESSING ROUTES LEADING TO HIGH-PERFORMANCE CERAMIC TILES

SUBJECT: Research Agreement No. DAAL03-88-K-0202

NAME OF INSTITUTION: State University of New York at Buffalo

AUTHORS OF REPORT: V. Hlavacek, S. Majorowski and J.A. Puszynski

Production of cheap high-performance ceramic tiles for structural application is an important problem. The search for superior tile exhibits many different facts ranging from establishing routes for manufacturing cheap precursors, through densification to ballistic testing of the material.

The main goals of the research sponsored by DARPA/BTI Project were:

- synthesis of ultrafine sinterable titanium diboride and titanium boride based composites in a combustion regime.
- purification of titanium diboride synthesized by magnesithermal reduction of boric and titanium oxides.
- densification and fabrication of TiB_2 based composites by pressureless sintering and hot pressing.
- ballistic testing of fabricated tiles.

1. Synthesis of ultrafine TiB_2 powder

There are several methods of TiB_2 synthesis:

- carbothermal reduction of TiO_2 in the presence of B_4C .
- synthesis of TiB_2 from gaseous precursors in plasma or aerosol generator.
- direct reaction between elements.

Accession For		
NTIS	CRA&I	<input checked="" type="checkbox"/>
DTIC	TAB	<input type="checkbox"/>
Unannounced		<input type="checkbox"/>
Justification		
By _____		
Distribution/		
Availability		
Dist	Accession of Special	
A-1		



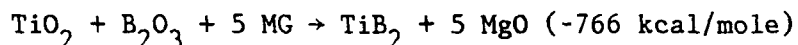
- synthesis of TiB_2 by magnesium thermal reduction of titanium and boric oxides.

The direct synthesis of titanium diboride from elements is not economically feasible due to the very high cost of boron powder. For the same reason the TiB_2 synthesized from gaseous precursors does not seem to be suitable for the manufacturing of cheap ceramic tiles. The TiB_2 powder obtained by carbothermal reduction of TiO_2 in the presence of B_4C is rather coarse and long milling times are required to reduce the particle size down to few microns. Unfortunately, further reduction is difficult due to the significant powder contamination. This powder cannot be pressureless sintered without metallic additives as chromium or nickel. These additives, significantly reduce ballistic performance of the tiles. The Laboratory for Ceramic and Reaction Engineering has developed the process for synthesis of ultrafine titanium diboride by magnesium thermal reduction of boric and titanic oxides in the combustion regime. The magnesiothermic reduction of titanium and boric oxides (4), is a strongly exothermic process. This reaction can be carried out in two regimes: kinetically or diffusionally controlled. The first one is characterized by slow reaction between TiO_2 , B_2O_3 and coarse (1-3 mm) Mg powder at temperatures below $1200^\circ C$ in an inert atmosphere. Diffusion of Mg into the oxide and chemical reduction kinetics control the process in this regime. In spite of a low reaction rate, its high parametric sensitivity may easily lead to spontaneous, uncontrollable combustion.

In a diffusionally controlled regime, chemical reaction once locally ignited by short duration energy pulse (resistively heated tungsten wire or chemical igniter) becomes a self-sustaining process which results in

formation of combustion front. The front propagation velocity and combustion temperature strongly depend on operating conditions such as bulk density, particle size, degree of dilution of the reactants and gas pressure, initial temperature and reactor configuration. However, information on magnesiothermic reduction in the self-sustaining regime is rather meager. In related systems, Cutler [1] have studied the sinterability of SiC synthesized by reduction of SiO₂ in the presence of C. Mamyan [2], based on thermodynamic analysis has found the optimum conditions for B₄C synthesis by reduction of B₂O₃. There are no reliable data on the magnesiothermic reduction of TiO₂ and B₂O₃ in the self-sustaining regime.

Titanium diboride was prepared by reduction of titanium and boric oxides in the presence of Mg according to the reaction:



Different TiO₂ powders from three sources: i) 17 μm¹ ii) 2 μm² iii) 0.3 μm³. Prior to ignition the reactants were properly blended, since the reaction rate critically depends on homogeneity. Vigorous mixing of both oxides with Mg powder has to be avoided due to possible self-ignition. Milling of TiO₂ with B₂O₃ (-325 mesh) for 4 hrs to obtain intimate contact between oxides, followed by gentle blending with Mg powder in the Turbula mixer gave the best results. Subsequently, the mixture has been poured into a graphite container and placed in a cylindrical, water

1 Alfa Products
2 Ferro Co.
3 Degussa Co.

cooled reactor operating under inert atmosphere. The reactor was evacuated down to 0.05 mm of Hg and filled with Ar to a desired pressure (1-100 atm). The mixture was ignited by a chemical igniter. The reaction was completed within few seconds. Cooled product was crushed and milled in a jar mill for 2 hrs.

A wide range of reactant particle sizes have been tested to synthesize ultrafine TiB_2 . The schematics of the channel reactor used in this study is shown in the Figure 1. The optimum combustion characteristics were accomplished by using fine (3-5 μm) Mg and TiO_2 powder with average particle size of 2 μm under 5 atm Ar pressure. The reduction process was relatively steady, with uniform combustion front propagation and without significant Mg evaporation. When coarser Mg powder was used (-200 + 325 mesh), the process was less stable, with hot spots forming in the combustion front and with more Mg evaporation and lower yield. For still coarser Mg (+100 mesh) the combustion process was not self-sustaining. Similar experiments with Mg having widely different particle size range have shown that the combustion front propagated in an unstable fashion. During the reduction, certain amount of Mg evaporated in spite of elevated inert gas pressure during the combustion. Therefore an excess of Mg in the initial mixture is required. Its amount depends on the inert gas pressure. At atmospheric pressure at least 10% excess of Mg above stoichiometric is needed, while under pressures above 10 atm (1-3%) excess is required.

Agglomerated TiB_2 was leached with HCl to remove MgO. For this, the product powder was fed into a water-containing leaching reactor equipped with a stirrer, cooling coil and a condenser. The weight ratio of water/powder should be more than two. Next, diluted HCl acid (10 wt%) was slowly pumped into the reactor.

Exothermic reaction between the MgO and HCl tends to raise the temperature, but 70°C was maintained by cooling, until all MgO was leached. The MgCl₂ solution was removed and leaching was repeated with more concentrated HCl acid (20 wt%), added in total volume 4l per kg of crude powder. During leaching, pH was controlled to minimize undesired reaction between TiB₂ and HCl. According to reported results [3] its rate is rather low at temperatures < 70°C. Leaching was carried out until pH = 5.5 was reached and did not change significantly over a period of 15 min. Then the solution was cooled and filtered. A wet cake was again dispersed in water by stirring for 1h at 70°C to dissolve any remaining MgCl₂. This operation was repeated using methanol instead of water at 50°C. Purified TiB₂ powder was then dried in vacuum and used for further studies.

TiB₂ synthesized by the above method was submicrometer in size, but formed agglomerates, some 2 μm in diameter. Typical particle size distribution and x-ray diffraction patterns powder are shown in Figs. 2 and 3. Specific surface area was 60 m²/g, a much higher value than 1 m²/g of TiB₂ from Union Carbide.

1.1. Photoelectron Spectroscopy

XPS analysis¹ of TiB₂ was done before and after hot pressing powdered TiB₂ into a dense body. The samples were irradiated under high vacuum (10⁻⁸ Torr) with Al Kα X-rays. The kinetic energy of the emitted photoelectrons, was measured according to $E_k = h\nu - BE - \phi_s + Y$ where $h\nu$ is the energy of the photons, BE is the electron binding energy, ϕ_s is the spectrometer work function and Y is the Volta potential due to charging of the sample. The

¹ Surface Science.

position of spectrum in respect to the kinetic energy shifts caused by instrumental effects (ϕ_s) was checked against an Au standard with Au 4f7/2 peak taken as 83.8 eV. Diborides are metallic so the intrinsic conductivity is expected to prevent steady-state charging. The charge was minimized by using flood gun at 2 eV. The main difficulty is choice of adequate reference level for the assignment of binding energies. The electron spectra were calibrated against reference carbon 1s line at 284.6 eV in the adsorbed hydrocarbon layer (ubiquitous carbon). Core level BE shifts can be caused by charging effects or by moving of the Fermi level. To get around such problems, core level BE separations between Ti and B or O 1s emissions were used. This allows easy checking of the crystalline states of the TiB_2 surface. The analyses were carried out on as-prepared powder, or in case of hot pressed TiB_2 , after sputtering away minimum of 1000 angstroms in depth to remove surface contamination. The photoelectron spectra were stored and deconvoluted into individual components as described later. Diborides were characterized by the ionization levels of their respective elements: 1s for B, O, N, and C, 2p 3/2 for Al and Ti. Peak intensities were integrated for elemental composition calculations. The pass energies used were 15 or 20 eV.

Due to the shallow penetration of soft X-rays, survey scans of as-prepared specimens invariably showed high oxygen and carbon concentration along with Mg and N impurities. Sputtering to depth of ~ 100 angstroms by a defocussed Ar beam of 5 KeV was used to remove oxide and hydrocarbon impurities from the hot pressed sample. In the electron emission spectrum of powder specimen, the dominant lines were Ti 2p, B 1s, O 1s, C 1s, N 1s and Mg 2p and Auger (KLL). The Auger line was analyzed. After hot

pressing, traces of Si, P and Al were detected at the surface, but were absent at a depth of 1000 angstroms.

1.1.1. Titanium

The separation between the binding energies of the Ti 2p_{3/2} and B 1s emissions were not identical in powder and in hot pressed TiB₂. They were 271.4 eV and 267 eV respectively, suggesting that hot pressing modified the chemical states of Ti and B atoms and affected core level BE's. This later value is very close to that of other diborides though (WZNB). Fig. 4 compares high resolution spectrum of Ti 2p emission from the powder with that of the hot pressed compact. Proximity of the maximum at BE of 458.7 eV to that of TiO₂ in the powder TiB₂, allows unambiguous assignment to oxide. Any emission due to Ti-B is masked by TiO₂. After hot pressing, the Ti 2p emissions shifted to lower BE and assumed asymmetrical distribution. The asymmetry and linewidth suggest that in addition to the main peak of Ti-B centered at 454.2 eV, another chemical component with a higher BE is present. TiO, TiC_x and TiOB_x are the most possible species for this BE of 455.4 eV. Also TiN with identical BE may be present since N 1s peak was detected as discussed later.

1.1.2. Boron

The B 1s electron spectra of TiB₂ consist of two and three components before and after HP respectively, with accompanying change of relative intensities, Fig. 5. The maximum located at about 187.2 eV is due to B-Me bond and is present in both materials. Its intensity substantially increased after hot-pressing. Component II, origin absent in the powder is shifted from the B-Ti emission in the HP diboride by about 1.6 eV, while component III at 192.2 eV, dominant in the powder, is reduced after hot

pressing. The later one corresponds to B^{+3-0} bonding in diboride and is identified as oxygen deficient B_xO_y .

1.1.3. Oxygen

The O 1s spectra from powder and TiB_2 are compared in Fig. 6. Asymmetry and line width of the O 1s peaks reveal presence of more than one chemical states of oxygen. Either two or three components are present in the powder and in the HP TiB_2 respectively. Deconvolution of these components shows that component II is shifted by 1.4-1.8 eV from the main emission. Component II, present only in the HP material, is shifted by .2.9 eV. The main component at 530.2 eV, present in both diboride forms, is due to O bonded with Ti rather than B. This is inferred from O 1s BE's for various metal oxides, generally being < 530.5 eV. Component II is tentatively assigned to B_xO_y and component III in HP TiB_2 may be related to TiO_x , MgO_x and NO_x .

1.1.4. Carbon

As mentioned before, C 1s spectra were used as a reference. In the powder, the strongest emission was assigned to ubiquitous C at 284.6 eV, so were the two emissions at 286.1 and 288.6 eV, Fig. 7. After hot pressing, these three components were also present, but an additional low energy tail developed at 282.2 eV, indicating appearance of Ti-C bonds. Notice that carbon species detected in hot pressed sample are incorporated into bulk structure. They persist after sputtering to ~ 1000 A, while adsorbed C is easily removed at much shallower depths, as for example observed in iridium.

1.1.5. Nitrogen

The N 1s emissions also suggest presence of various chemical species in the diboride. Two emissions at 396.7 eV and 400 eV are present in both

materials, the third one at 398.3 eV appeared after hot pressing and close to that of BN.

1.1.6. Magnesium

In both TiB_2 forms, the Mg (KLL) Auger emissions were centered around 306 eV and were quite similar.

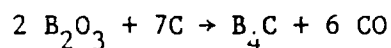
XPS spectroscopy showed that substantial differences exist among chemical species present in the powder and in hot pressed TiB_2 forms. The binding energies for the two cases are summarized in Table II. By comparison with the BE's of the known compounds, identification of chemical species can be made and the reaction sequences described. As expected for fine TiB_2 powder, which is pyrophoric, a layer of TiO_x and B_xO_y is formed in air environment at room temperature. It is unlikely that these are unreacted remnants of reactants. Ubiquitous carbon species (hydrocarbons) are also adsorbed on the surface upon exposure to atmosphere. Other impurities were N and Mg.

These surface species react and form new compounds during densification at elevated temperatures. This is evidenced by BE shifts and appearance of additional components in the hot pressed diborides. Oxides, carbides and nitrides presumably form and are responsible for multicomponent, C and N 1s emissions. Inspection of Ti-B-C phase diagram reveals that at 2000°C stoichiometric TiB_2 coexists with C. TiB_2 with slight B deficiency is in equilibrium with TiC, while that with B excess coexists with B_4C (WW). Mg emissions indicates presence of MgO or MgB_x . The fact that leaching did not remove Mg entirely suggests that residual Mg is combined, possibly as a solid solution with TiB_2 .

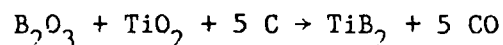
Considerable work has been done on understanding sintering mechanisms in TiB_2 . Although a great deal remains to be learned, it is known that

removal of oxygen from grain boundaries is essential for densification. Redox equilibria have a profound effect on sintering process. B_2O_3 is a glass former with melting point of $450^\circ C$. Therefore it is likely that as the sintering temperatures of $1600^\circ C$ to $2000^\circ C$ are approached, B_2O_3 first dissolves TiO_x and then vaporizes, enriching the grains with TiO_x . Such oxidation mechanism was documented for ZrB_2 . Since oxides and borides are not readily compatible, densification is retarded. It suffices to say that C inhibits grain growth and promotes densification by inhibition of pore entrapment. In this context stability of B_2O_3 glass in reducing conditions and the role of C in removing oxygen needs to be considered.

Presence of C may promote the reactions:



and



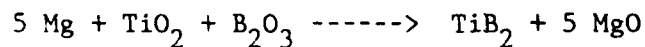
The first reaction removes the glass phase and enriches boron content of the system. The second one is actually carbothermic synthesis process.

It is expected that during sintering and hot-pressing, which is usually carried out in a graphite lined furnace, the oxides formed during atmospheric exposure are either reduced or form oxyborides. In fact, transmission electron microscopy studies of several dense TiB_2 did not show presence of intergranular liquid phase which could be associated with B_2O_3 , suggesting that above reactions are taking place.

In order to minimize oxygen content, the powder would need to be handled under protective atmosphere during entire processing cycle, from synthesis until densification, a rather impractical undertaking. Although the oxide layer is not thicker than 50-100 angstroms, and therefore constitutes only about 3% of a $1 \mu\text{m}^3$ volume grain, for a powder with a high surface area, the amount of oxides can be substantial. Alternatively, addition of small amounts of carbon prior to sintering assist in eliminating the oxygen. It remains to determine quantitatively the optimum amount of required carbon additions. When excess of carbon is used, TiC precipitates may form during processing, and their presence is probably advantageous in improving the high temperature creep resistance (WW). For applications as electrodes for aluminum industry however, TiC traces are highly undesirable due to its rapid reaction with aluminium and formation of Al_4C_3 and TiAl_3 . Al_4C_3 is unstable in humid environments, decomposes to $\text{Al}(\text{OH})_3$ and C_2H_2 , and the electrode slowly desintegrates to powder.

Economical Outlook of Magnesumthermal Reduction of Boric and Titanium Oxides

The magnesumthermal reduction reaction of TiO_2 and B_2O_3 is written:



In order to obtain 1lb of titanium diboride the amounts of 1.98lb of magnesium (3-5% excess is required), 1.27lb of titanium dioxide and 1.1lb of boric oxides have to be required (based on usual 90% yield of the overall process). In order to estimate the cost of our titanium diboride we contacted different manufacturers of magnesium, titanium dioxide and boric

oxide powders. The current prices (in a large quantities) of magnesium powder from ESM Company are:

powder (-325 mesh) \$8.25/lb

powder (-200 mesh) \$6.40/lb

powder (-100 mesh) \$2.60/lb

Other manufacturers like READE Co., HART METALS Inc. or KLM METALS Inc. have prices approximately 20% higher.

We have found that titanium dioxide from FERRO Co. (average particle size $\sim 2 \mu\text{m}$) is sold for \$2.50/lb. Submicron titanium dioxide supplied by DEGUSSA Co. is expensive (\$14/lb.)

The cost analysis for two different prices of magnesium powder is presented in the Table 1.

TABLE 1. Estimation of titanium diboride unit cost.

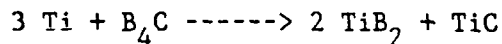
<u>CHEMICALS</u>	<u>UNIT PRICE</u>	<u>TOTAL PRICE</u>
1.98 lb of Mg	\$8.25/lb (\$2.60/lb)	\$16.34 (\$5.15)
1.27 lb of TiO_2	2.50/lb	3.18
1.10 lb of B_2O_3	1.50/lb	1.65
6.61 of HCl (20°)	0.1/lb	<u>0.66</u>
	TOTAL	\$21.83 (\$10.64)

From this analysis it can be seen that it is possible to obtain ultrafine titanium diboride for the price close to \$10/lb when the magnesium fine powder would be supplied at the same price as a magnesium powder (-100 mesh). It is also another possibility to reduce the overall cost of the powder. The partial preheating of the reacting mixture might be a

sufficient effort in order to make the magnesium powder (-100 mesh) a good reducing agent for SHS process.

DIRECT REACTION BETWEEN TITANIUM AND BORON CARBIDE

Definitely from the economical point of view the synthesis of powdered titanium diboride from elements is unjustified; however, the synthesis of TiB_2 -TiC composite from Ti powder and boron carbide is very promising. The current price of a fine boron carbide $d_{av} < 7 \mu m$ is ~\$25/lb. The price of titanium powder (-325 mesh) is \$15/lb. The cost of TiB_2 /TiC composite synthesized in the combustion regime, accordingly to the reaction scheme:



is approximately \$18/lb compared to \$15/lb of the mix prepared from TiB_2 and TiC and more than \$30/lb of that obtained in direct reaction between titanium, boron and carbon.

The reaction between boron carbide and titanium metal is strongly exothermic and generates temperatures in the excess of 2500°C. We feel that this reaction has a potential application in the process of the simultaneous synthesis of TiB_2 -TiC composite and its densification. In order to ignite Ti - B_4C system a very fine boron carbide powder is required ($d_{av} < 10 \mu m$). We have found that the mixture of titanium powder (-325 mesh) and boron carbide ($d_{av} < 7 \mu m$) exhibits the best ignition and combustion front characteristics. We have found that standard grade of boron carbide which is commercially available is not suitable for this process. It is necessary to reduce the particle size of that boron carbide grade by attrition milling using iron beads and subsequently leaching of iron by diluted hydrochloric

acid. Boron carbide purchased from ESK Company ($d_{av} = 15 \mu\text{m}$) was milled in the attritor for 2, 3, and 5 hours. It was found that at least 3 hrs milling time is required to reduce the average particle size below $10 \mu\text{m}$. In order to avoid any partial melting or sintering of the product some dilution 10-20% by weight is recommended. The combustion product was milled for 4 hrs. in the jar mill with alumina balls to break the agglomerates which were formed during the synthesis. The average particle size of the product was $3.2 \mu\text{m}$. The phase composition is shown in the Fig. 8.

In order to reduce further the average particle size down to $1.5 \mu\text{m}$ for the pressureless sintering TiB_2/TiC composite material was milled in attritor for 6-8 hrs.

DENSIFICATION AND FABRICATION OF TITANIUM DIBORIDE BASED COMPOSITES

Major efforts have been directed towards pressureless sintering of the synthesized compositions in addition to conventional hot-pressing. It was our understanding that pressureless sintering, all other things being equal, would be the most competitive from the economical point of view. For these reasons we developed a number of sinterable TiB_2 based compositions: $\text{TiB}_2\text{-AlN}$ and $\text{TiB}_2\text{-TiC}$. Aluminum nitride based composites can be sintered up to 95% density within the range of TiB_2 content from 0 to 70%. Another material- $\text{TiB}_2\text{-TiC}$ obtained by SHS synthesis is also sinterable (density 98% of theoretical at 2000°C). Ballistic target made from this composite material has been already submitted for testing.

During the duration of the project we devoted considerable efforts to large scale processing of the powders (synthesis, milling, cold and hot-pressing, binder removal, sintering).

We gained substantial expertise in the area of the scale-up of certain SHS processes. The process of fabrication of standard 4 x 4 x 1/2 ballistic targets has been developed. As a result we are currently capable of synthesizing and ballistic testing of almost any SHS synthesized material.

BALLISTIC TESTING OF FABRICATED TILES

A number of tiles (4" x 4" x 1/2") has been fabricated by pressureless sintering or hot pressing. They have been submitted for testing to the Impact Physics Laboratory, University of Dayton Research Institute.

Fig. 9 compares the performance of our AlN tile with other ceramics. The x-axis is tile aerial density (w_c). The y-axis is the penetrated weight in the substrate (w_r). Since the penetration was incomplete, the aerial density of unpenetrated tile was entered as a negative number. For most materials the w_r data should fall on a straight line. Failure to get complete tile penetration ($w_r < 0$) is essentially an off-scale result in this type of test. Thus, the conclusion can be made that this is a very competent ceramic, since the steel core shattered (usually half the core penetrates), and had we tested a thicker sample, it would probably have done better than a good ballistic alumina.

The other mixes: #1 (50% TiB_2) and #2 (20% TiB_2 in AlN) were shot with a tungsten bullet. This bullet simulates a future competent anti-armor threat. Fig. 10 shows the results. The material performed competitively with hot pressed TiB_2 and SiC. According to Dr. S. Bless from the Impact Physics Laboratory, the results look very encouraging. Additional tests (TiB_2 -TiC) are under way.

References

1. R.A. Cutler; "Synthesis of Submicron Silicon Carbide," DARPA/ARMY SHS Proceedings, Daytona Beach 75, (1985).
2. S.S. Mamyán; "A Study of the Possibility of Producing Boron Carbide Powder by the Method of SHS with Reducing Step," Probl. Tekhnol. Goreniya. Materialy 3-1 Vses. Konf. po Tekhnol. Goreniya 17, (1981).
3. I.D. Chausskaya and L.V. Kustova; "Extraction of Titanium Diboride from Combustion Products in an SHS Process with Reduction Step," Probl. Tekhnol. Goreniya. Materialy 3-1 Vses. Konf. po Tekhnol. Goreniya 44, (1981).

Table II
 Comparison of measured binding energies (eV)
 (Corrected against C 1s emission)

		<u>Ti 2p_{3/2} lines</u>		
	I	I-I	Ti 2p-B 1s	
TiB ₂ powder	458.7	-	271.4	
hot pressed	454.2	1.2	267.0	
		<u>B 1s lines</u>		
	I	II-I	III-I	
TiB ₂ powder	187.3	-	5.0	
hot pressed	187.2	1.6	4.9	
		<u>C 1s lines</u>		
TiB ₂ powder	284.6	1.5	4.0	
hot pressed	284.6	1.6	4.2	-2.4
		<u>O 1s lines</u>		
TiB ₂ powder	530.1	1.8	-	
hot pressed	530.4	1.4	2.9	
		<u>N 1s lines</u>		
TiB ₂ powder	396.7	-	3.3	
hot pressed	396.7	1.6	3.3	
		<u>Mg Auger</u>		
TiB ₂ powder	305.1			
hot pressed	306.4			

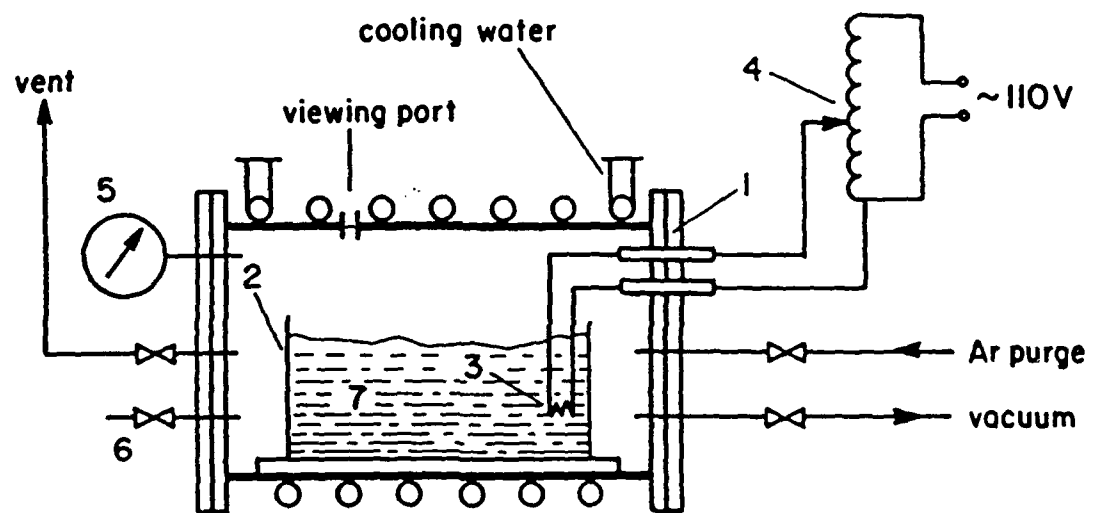


Figure 1. Schematics of cylindrical reactor used for magnesothermal synthesis. 1- reactor, 2- graphite container, 3- igniter, 4- transformer 5- pressure gauge, 6- safety valve, 7- reactants charge.

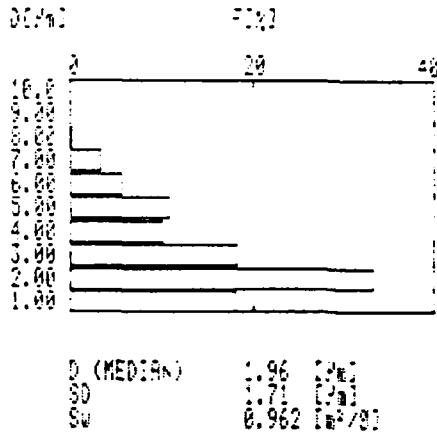


Fig. 2 The particle size distribution of ultrafine TiB_2 powder.

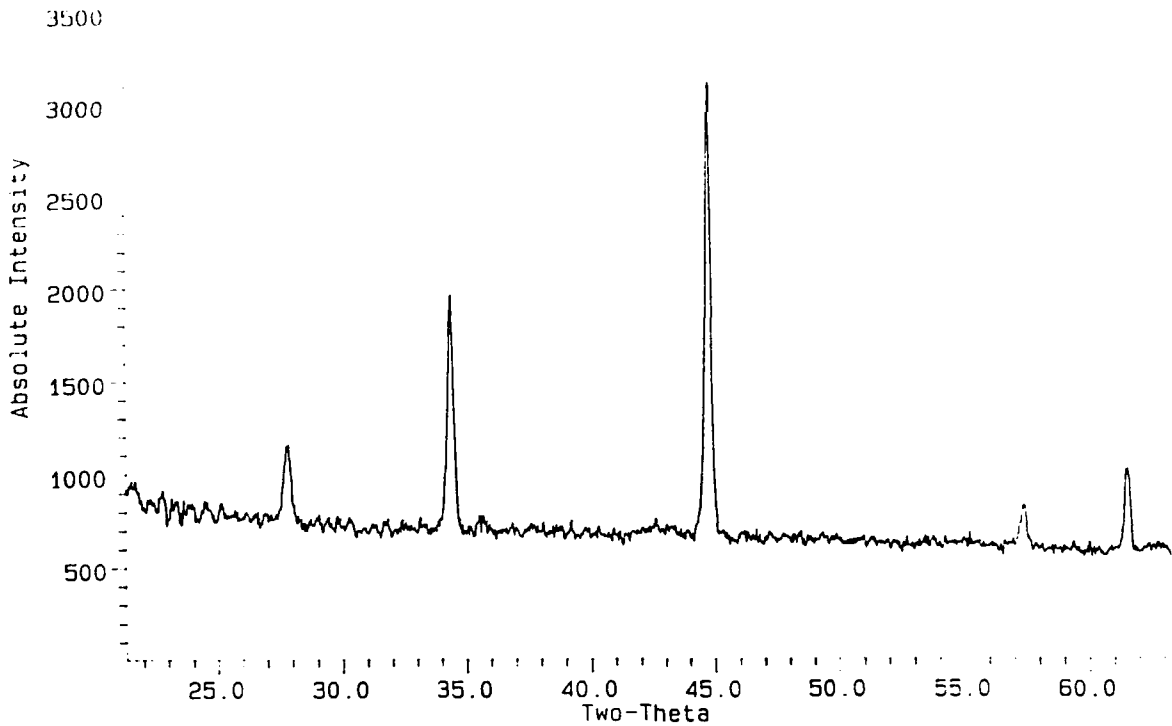


Figure 3. X-RAY patterns of TiB_2 synthesized by magnesothermal reduction of titanium and boric oxides in a combustion regime.

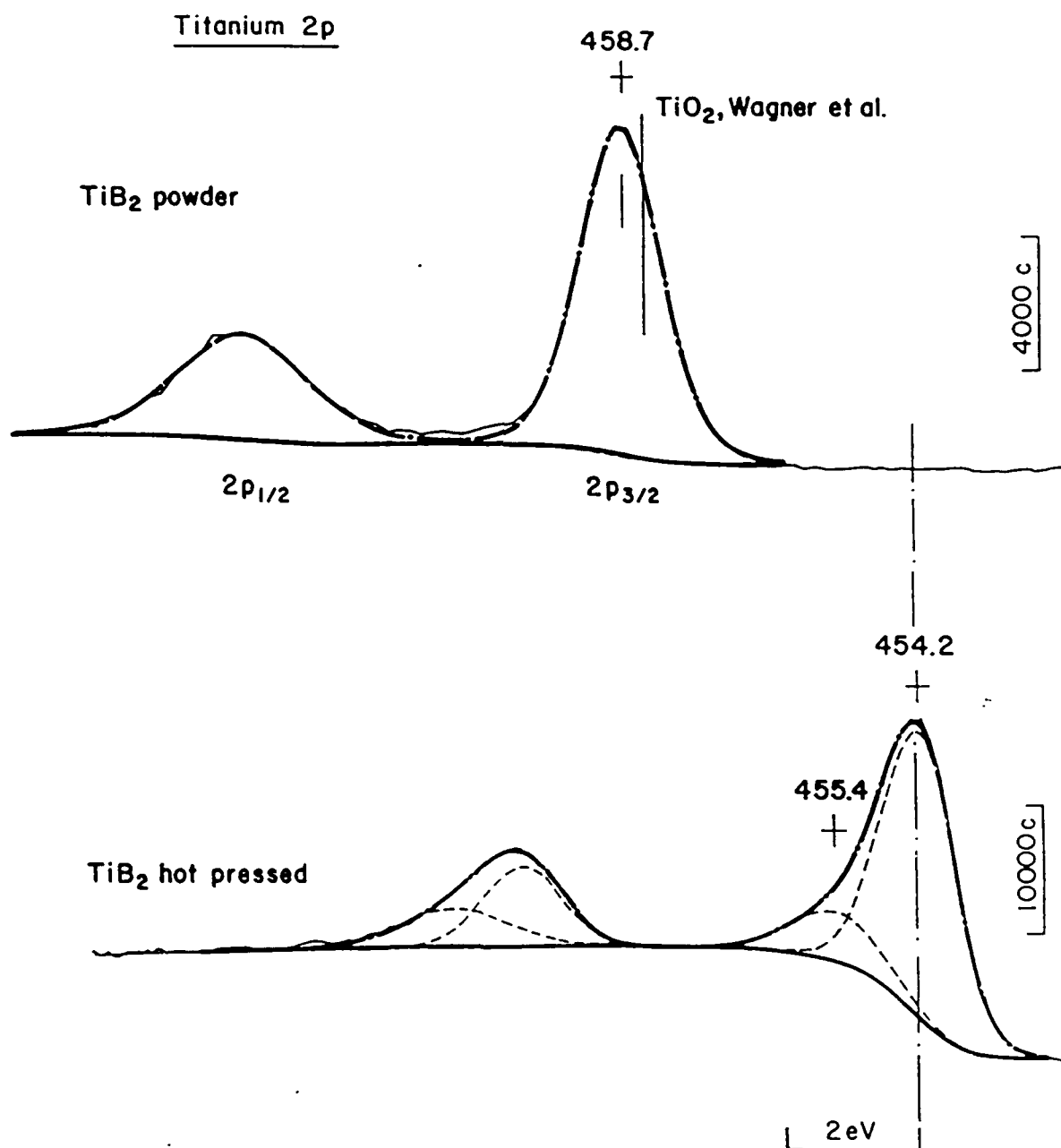


Figure 4. Titanium 2p emissions of synthesized TiB₂ powder (surface) and hot-pressed TiB₂ (after sputtering).

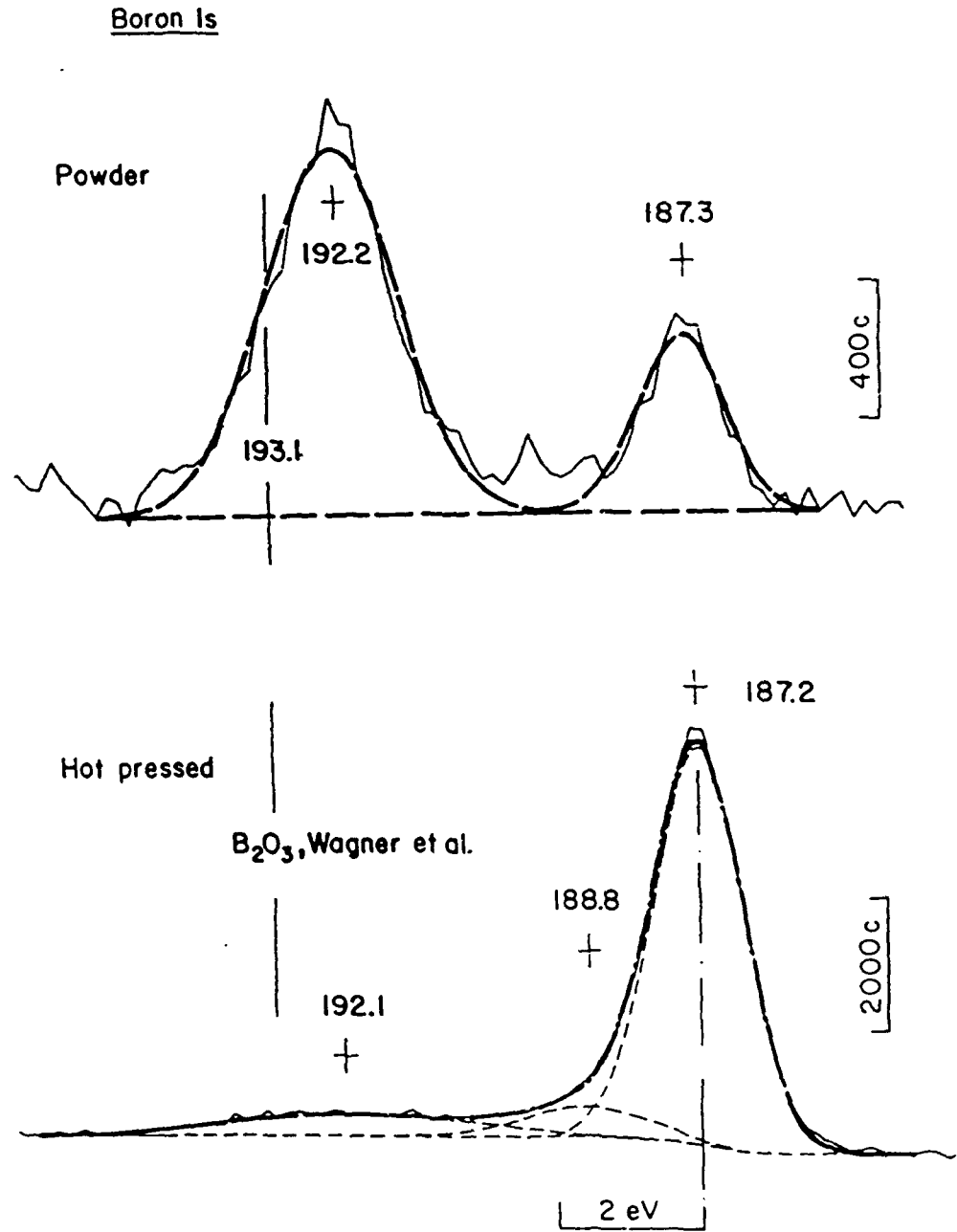


Figure 5. Comparison of B 1s emissions in both TiB_2 forms.

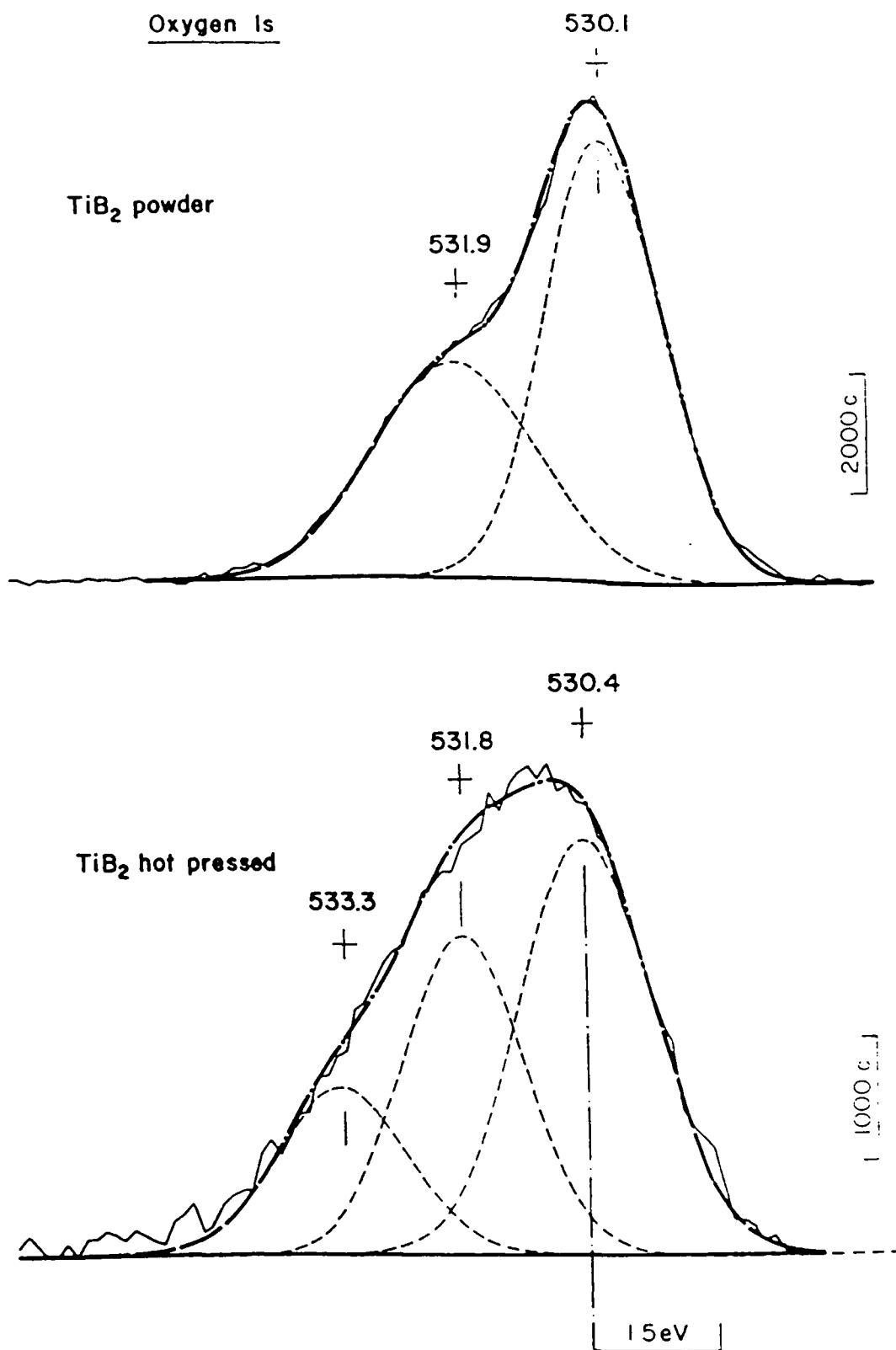


Figure 6. Comparison of O 1s emissions in powder and hot-pressed TiB₂.

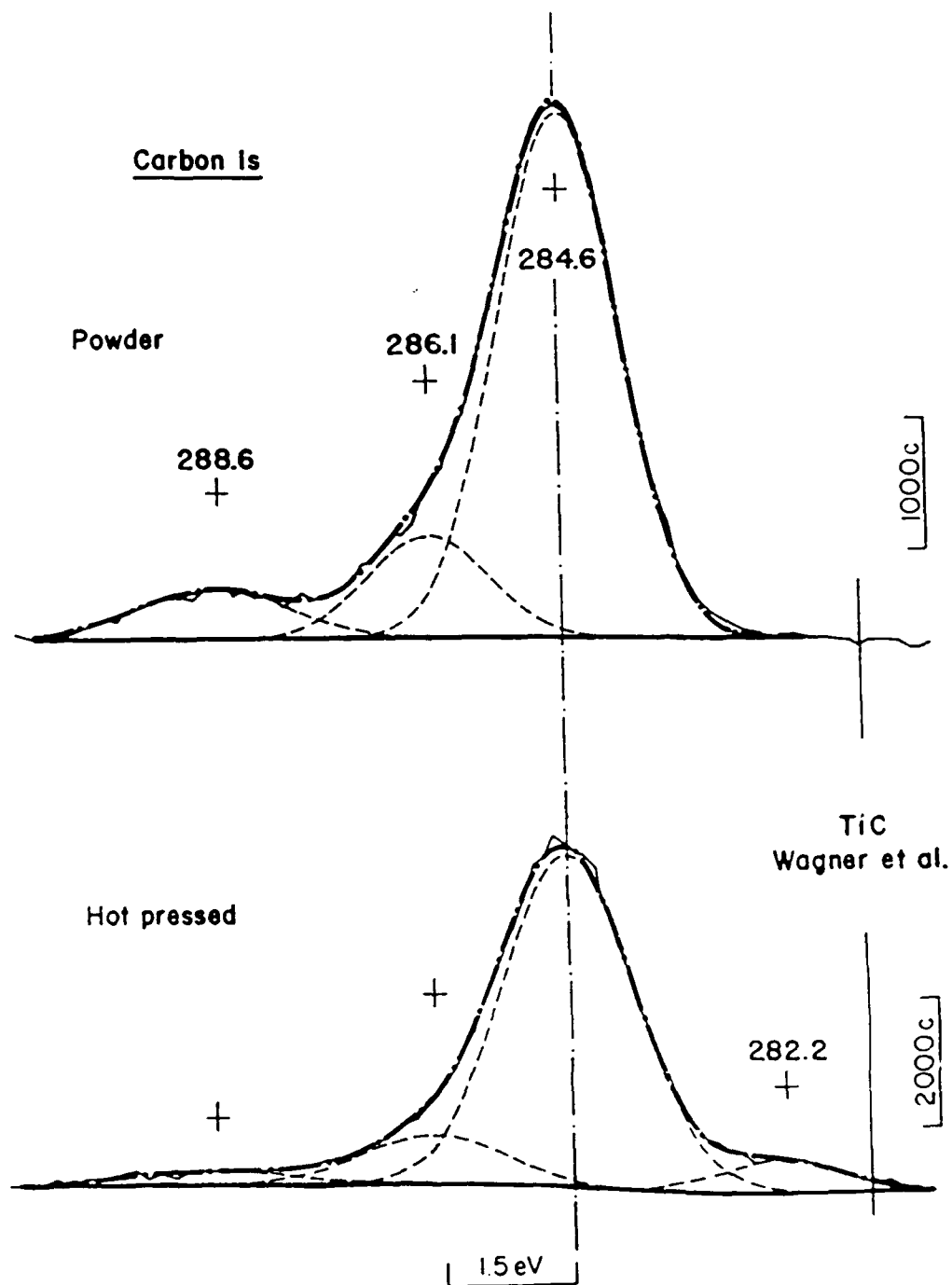


Figure 7. Comparison of C 1s emissions in powder and hot-pressed, 1000A sputtered TiB_2 . In pure Cu clean C surface is obtained at depth of 60A.

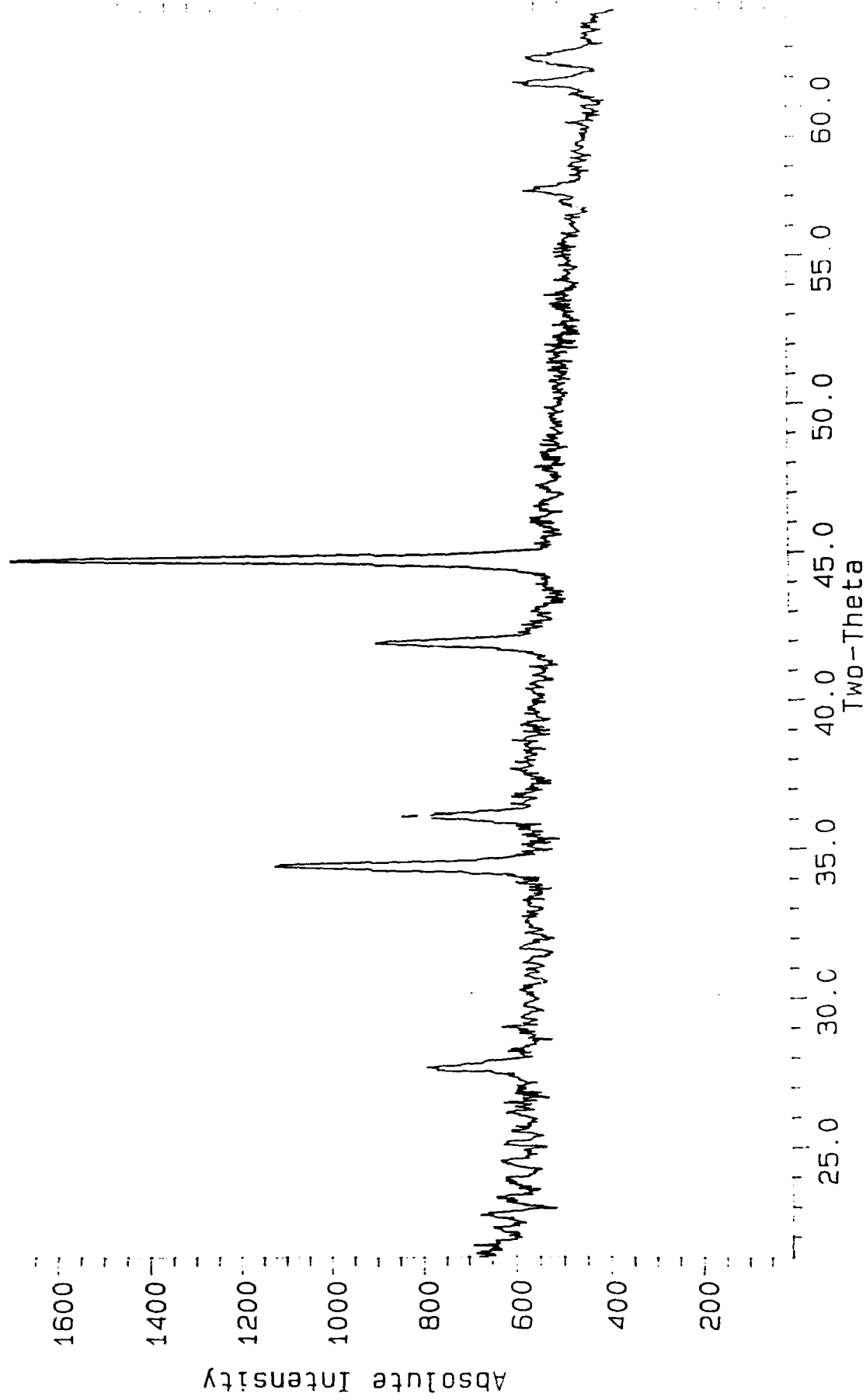


Figure 8. X-Ray diffraction patterns of TiB₂-TiC from combustion synthesis.

11-4-3

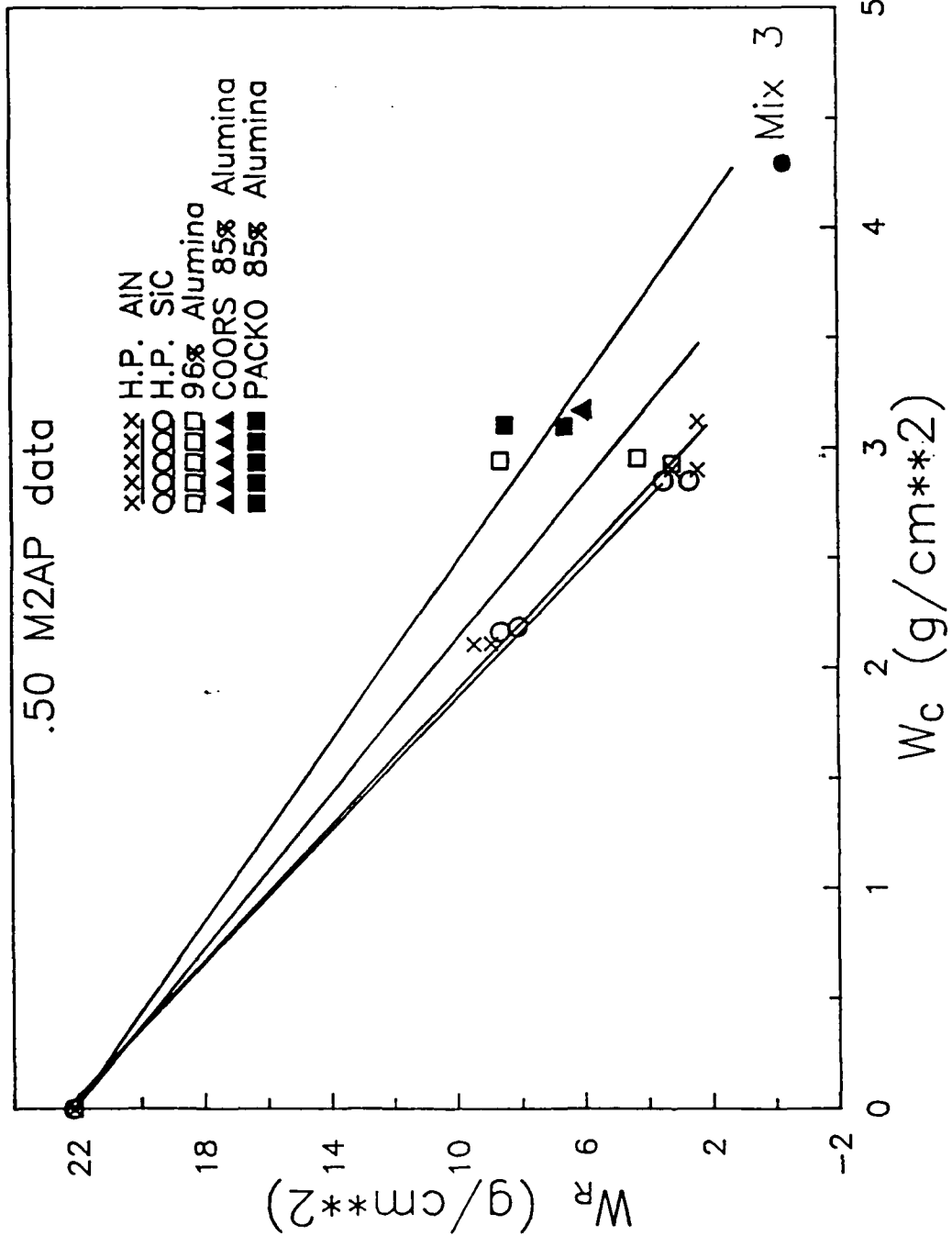


Figure 9. Ballistic performance of AlN tile with other ceramics.

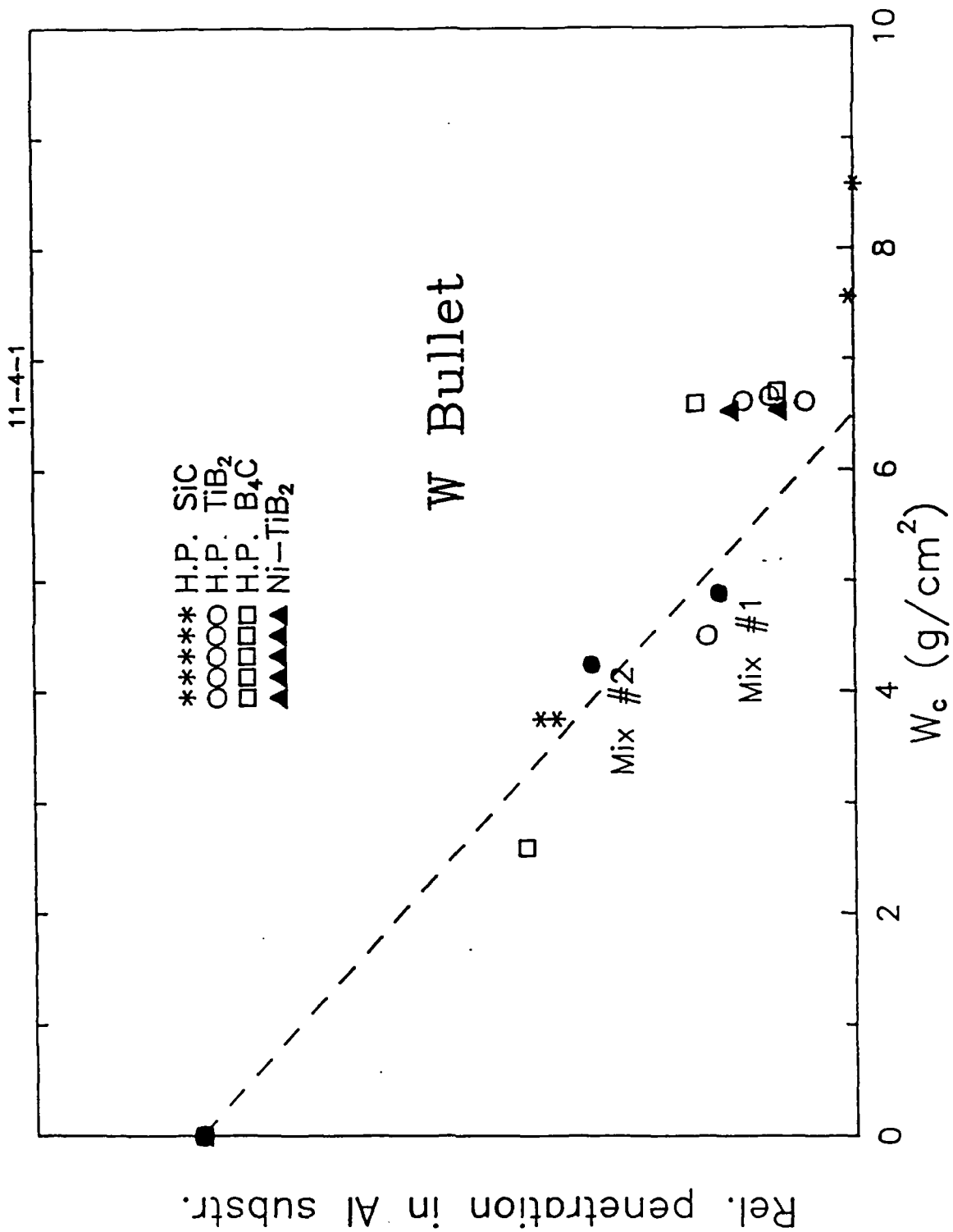


Figure 10. Ballistic performanc of TiB₂-AlN tiles. Mix #1 (50% of TiB₂), Mix #2 (20% of TiB₂)